MOLECULAR AND CELLULAR BIOLOGY, Aug. 2002, p. 5527–5538 Vol. 22, No. 15
0270-7306/02/$04.00+0 DOI: 10.1128/MCB.22.15.5527–5538.2002

Mdm4 (Mdmx) Regulates p53-Induced Growth Arrest and Neuronal Cell Death during Early Embryonic Mouse Development

Domenico Migliorini,[1] Eros Lazzerini Denchi,[1,2] Davide Danovi,[1] Aart Jochemsen,[3] Manuela Capillo,[2] Alberto Gobbi,[2] Kristian Helin,[1,2] Pier Giuseppe Pelicci,[1,2]* and Jean-Christophe Marine[1]*

Department of Experimental Oncology, European Institute of Oncology, 20141 Milan,[1] and The FIRC Institute of Molecular Oncology, 20139 Milan,[2] Italy, and Department of Molecular and Cell Biology and Center for Biomedical Genetics, Leiden University Medical Center, 2300 RA Leiden, The Netherlands[3]

Received 15 January 2002/Returned for modification 15 February 2002/Accepted 25 April 2002

We report here the characterization of a mutant mouse line with a specific gene trap event in the *Mdm4* locus. Absence of Mdm4 expression results in embryonic lethality (10.5 days postcoitum [dpc]), which was rescued by transferring the *Mdm4* mutation into a *Trp53*-null background. Mutant embryos were characterized by overall growth deficiency, anemia, improper neural tube closure, and dilation of lateral ventricles. In situ analysis demonstrated increased levels of $p21^{CIP1/Waf1}$ and lower levels of *Cyclin E* and proliferating cell nuclear antigen expression. Consistent with lack of 5-bromo-2′-deoxyuridine incorporation, these data suggest a block of mutant embryo cells in the G_1 phase of the cell cycle. Accordingly, Mdm4-deficient mouse embryonic fibroblasts manifested a greatly reduced proliferative capacity in culture. Moreover, extensive p53-dependent cell death was specifically detected in the developing central nervous system of the *Mdm4* mutant embryos. These findings unambiguously assign a critical role for Mdm4 as a negative regulator of p53 and suggest that Mdm4 could contribute to neoplasias retaining wild-type *Trp53*. Finally, we provide evidence indicating that Mdm4 plays no role on cell proliferation or cell cycle control that is distinct from its ability to modulate p53 function.

In cells exposed to various forms of stress, the p53 protein is stabilized and consequently elicits either cell cycle arrest or apoptosis, thereby protecting organisms from developing cancer (16). The central role of the *Trp53* gene in tumor suppression is underscored by the fact that half of human cancers have *Trp53* mutations (16), whereas the remainder exhibit genetic or functional inactivation of genes, which disable p53 function. The Hdm2 oncoprotein is a critical negative regulator of p53, which directly blocks its transcriptional ability and stimulates its nuclear export and proteolytic destruction (3, 7, 27, 35). Hdm2 functions as an E3 ubiquitin ligase for p53, and the C-terminal Ring finger domain of Hdm2 is critical for ligase activity (3, 7). Interestingly, the *Hdm2* gene itself is a transcriptional target of p53. Thus, there is evidence for an autoregulatory feedback loop involving the expression and function of Hdm2 and p53. From a genetic standpoint, the functional relationship between the mouse ortholog of *Hdm2*, *Mdm2*, and *Trp53* is supported by the observation that a p53-null state completely rescues the early embryonic-lethal phenotype associated with *Mdm2* deficiency (12, 20).

Mdm4 is structurally related to Mdm2, binds to p53, and inhibits transactivation in vitro, but unlike Mdm2, is unable to induce p53 degradation (11, 30–32). Mdm4 and Mdm2 form stable heterodimers through their C-terminal Ring finger domains, and this interaction results in a substantial increase in the steady-state levels of Mdm2 (29, 34). Ectopic expression of Mdm4 (or Hdm4) interferes with Mdm2-mediated p53 degradation, resulting in increased p53 protein levels. Recently, it has been proposed that Mdm4 stabilizes Mdm2 and p53 through distinct mechanisms (18, 33). Mdm4 expression reverses Mdm2-mediated p53 nuclear export and leads to accumulation of ubiquitylated, nuclear p53 without significantly affecting Mdm2-mediated ubiquitylation of p53. In contrast, Mdm4 stabilizes Mdm2 by inhibiting its self-ubiquitylation (33). The biological significance of these activities remains to be elucidated.

Mutation of *Mdm4* has been recently reported to cause p53-dependent embryonic lethality in mice, essentially due to severe proliferation defects (25). The absence of apoptosis in these mutants led to the hypothesis that Mdm4 selectively inhibits the ability of p53 to induce growth arrest; Mdm2 would, instead, regulate the apoptotic function of p53. We report here another *Mdm4* mutant generated by insertional mutagenesis, which also leads to a p53-dependent embryonic lethality, but with striking phenotypic differences such as later embryonic lethality and evidence of massive apoptosis in the developing central nervous system (CNS). These data support a direct role for Mdm4 in regulating both apoptotic and cell cycle arrest functions of p53. Furthermore, we present evidence suggesting that deletion of Mdm4 has no additional effect on cell proliferation or cell cycle control when p53 is absent.

* Corresponding author. Mailing address for Jean-Christophe Marine and Pier Giuseppe Pelicci: Department of Experimental Oncology, European Institute of Oncology, 435 Via Ripamonti, 20141 Milan, Italy. Phone: 39 0257489834. Fax: 39 0257489851. E-mail address for Jean-Christophe Marine: cmarine@lar.ieo.it. E-mail address for Pier Giuseppe Pelicci: pgpelicci@ieo.it.

MATERIALS AND METHODS

Generation of the Mdm4-deficient mice. An ES clone with a single gene trap event in the *Mdm4* locus was used to generate the *Mdm4*-deficient mouse line (38). The vector used to create this particular ES cell clone was VICTR49 (5.1

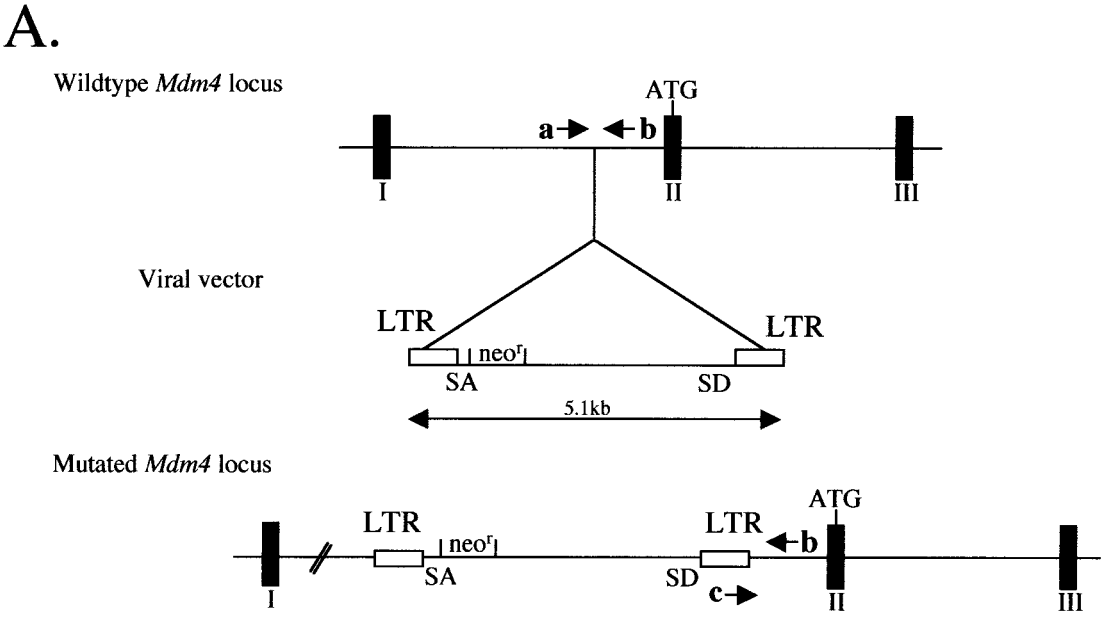

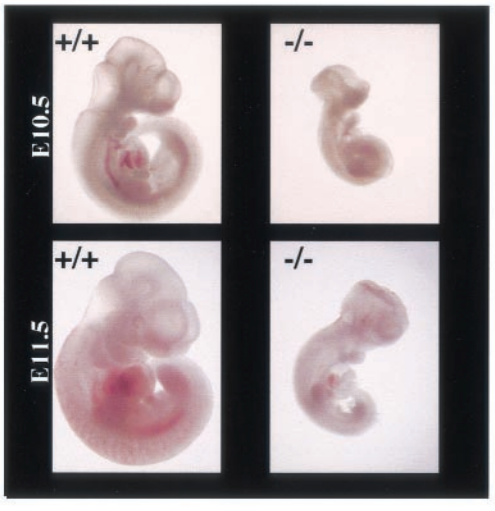

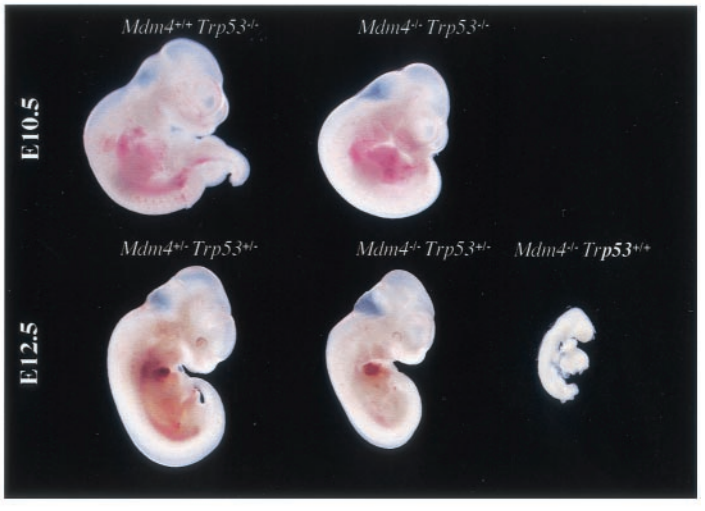

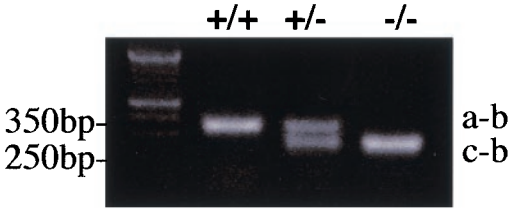

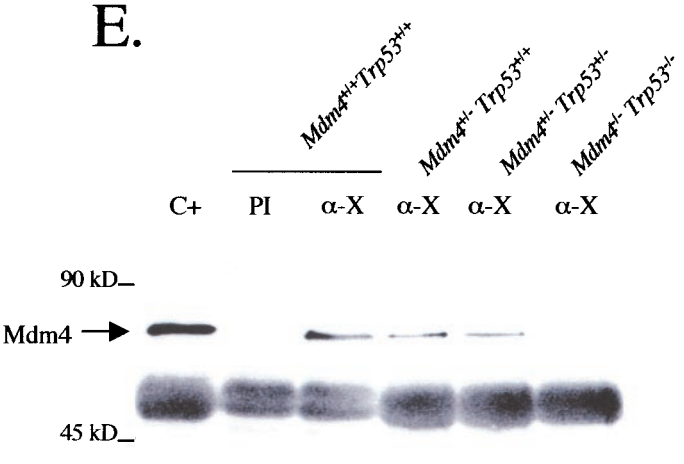

TABLE 1. Genotyping analysis of progeny from *Mdm4* heterozygous intercrosses

Stage	No. of litters	Total no. of embryos	No. of embryos with *Mdm4* genotype			No. with growth defect/abn.[a]	−/− (%)[b]	No. of resorbing embryos[c]
			+/+	+/−	−/−			
E9.5	2	14	6	4	4	3	29	0
E10.5	2	17	3	10	4	4	24	0
E11.5	6	49	14	24	11	9	18	2
E12	2	16	2	7	5	1	6	4
E12.5	2	15	6	8	1	0	0	1
E13.5	3	22	5	16	0	0	0	0
F2	12	88	32	56	0			

[a] Number of embryos with a growth defect or abnormality.
[b] Percentage of embryos with *Mdm4*$^{-/-}$ genotype.
[c] All resorbing embryos were identified as *Mdm4* homozygous mutants

kb) containing a splicing acceptor site (SA), a Neo^r cassette for positive selection and the splicing donor site (SD) of the first exon of the *BTK* gene. To precisely locate the insertion site of the trapping vector, a PCR fragment was amplified, using primers at the 3′end of the retroviral vector (5′-GTCTGGGGAGCTAC CTGC) and in the second intron of the *Mdm4* locus (5′-GACAAGCAGAAG GGCACAAAC), cloned, and sequenced. The insertion occurred 194 bp upstream of exon II (see Fig. 1A).

PCR genotyping. A PCR-based strategy was developed to distinguish between the wild-type and *Mdm4* mutant alleles. The primers are as follows: a, 5′-TAG GTTCAATTCCTGCAGCCC; b, 5′-GAGAATTTCAGTTCAGTGTGAGT; c, 5′-GCCTTGCAAAATGGCGTTACTT (see Fig. 1A). A 250-bp fragment indicates the presence of the mutated allele, whereas a 350-bp fragment is amplified from the wild-type allele (see Fig. 1B). Trp53 genotyping was determined as previously described (10).

Histology. For sectioning, embryos were fixed in 4% paraformaldhehyde–1× phosphate-buffered saline (PBS) overnight, embedded in paraffin, sectioned, and stained in hematoxylin and eosin.

In situ hybridization (ISH), 5-bromo-2′-deoxyuridine (BrdU), and immunohistochemistry. RNA in situ hybridization was carried out essentially as previously described (1), using [α-^{32}P]-UTP-labeled antisense cRNA probed transcribed from plasmids containing murine cDNA fragments of *Mdm4*, *Cyclin E*, and *p21^{Waf1}*.

For BrdU experiments, pregnant females were injected intraperitoneally with 100 μg of BrdU/g of body weight and sacrificed 2 h later.

The following antisera were used: biotinylated anti-proliferating cell nuclear antigen (anti-PCNA) (1/200; Pharmingen), anti-BrdU (1/200; Boehringer Mannheim), anti-cleaved caspase 3 (1/200; Cell Signaling), and anti-phosphorylated histone H3 (PH3) (1/200; Upstate). Except for the PCNA staining, an appropriate biotinylated secondary antibody immunoglobulin G was then applied to the slides. Avidin-conjugated peroxidase (ABC and DAB kits from Vector Laboratories) was used for immunostaining.

Immunoprecipitation and Western blotting. Adult brains of the appropriate genotype were smashed through a cell strainer (70-μm pore size; Becton Dickinson) in ice-cold PBS. Cells were washed twice in 1× PBS. The cells were lysed in a solution containing 50 mM HEPES (pH 7.5), 150 mM NaCl, 1 mM EDTA, 2.5 mM EGTA, 2 mM dithiothreitol, 0.1% Tween 20, 1 mM phenylmethylsulfonyl fluoride, 0.4 U of aprotinin per ml, 10 mM β-glycerophosphate, 1 mM NaF, and 0.1 mM $NaVO_4$. The cells were sonicated three times for 10 s with a sonicator (ultrasonic processor XL; Heat Systems) (12 to 14% power). Immunoprecipitation experiments were performed on 2 mg of brain extract using rabbit polyclonal anti-Mdm4 antibodies p55 and p56 raised against full-length recombinant Mdm4 and SI23 raised against two peptides chosen in the central portion of the protein (amino acids 142 to 156 and 268 to 281). Mdm4 was detected using a 1/3 dilution mixture of the hybridoma supernatants 6B1A (recognizing an epitope in the central portion of the protein) and 11F4D (recognizing an epitope in the Ring finger domain of Mdm4) (25, 33). This particular combination of antibodies ensures detection of all possible Mdm4 protein variants.

For direct Western blotting analysis, mouse embryonic fibroblasts (MEFs) were prepared and lysed as described above. The protein concentration was determined by Bradford assay, and 75 μg of each extract was fractionated by sodium dodecyl sulfate-polyacrylamide gel electrophoresis and transferred to nitrocellulose. The antibodies used were as follows: anti-p53 sheep polyclonal Ab-7 (1/500; Oncogene), anti-p21 rabbit polyclonal F5 (1/500; Santa Cruz), antivinculin mouse monoclonal antibody, clone hVIN-1, (1/1,000; Sigma) for normalization.

Immunofluorescence. For immunofluorescence staining, cells were plated on glass coverslips in 12-well dishes and fixed 10 min in 4% paraformaldhehyde–1× PBS. Fixed coverslips were washed twice in PBS, permeabilized in 0.15% Triton X-100 for 5 min, and incubated in blocking buffer (PBS with 2% bovine serum albumin) for 30 min. Cells were then incubated in blocking buffer containing primary antibody (anti-p53 rabbit polyclonal antibody CM5; Novocastra Laboratories, Ltd.) for 1 h and then washed extensively in PBS before incubation with the appropriate fluorochrome-conjugated secondary antibody. Stained cells were mounted on glass slides and examined by standard immunofluorescence microscopy.

Tissue culture assays. Cells were maintained in Dulbecco modified Eagle medium supplemented with 10% fetal bovine serum (FBS) (Gibco). Mouse embryonic fibroblasts were prepared from embryos at embryonic day 10.5 (E10.5). The head and organs were dissected, and fetal tissue samples were rinsed in PBS, minced, and trypsinized for10 min at 37°C, and subsequently dissociated in medium. The cells were then plated out into 12- or 6-well plates. These cells were considered passage 1 MEFs.

For growth curves, 2.5×10^4 or 5×10^5 cells were either plated in duplicate into 12-well plates or 10-cm-diameter dishes, respectively. At various time points, cells were trypsinized and counted.

FIG. 1. A gene trap event in the *Mdm4* locus leads to a null *Mdm4* mutation and early embryonic lethality in mice. (A) The structure and size of the retroviral construct along with the structures of the wild-type and mutated alleles and the positions of the oligonucleotides used for the PCR-based strategy are depicted. Exons (black vertical bars) and the long terminal repeats (LTRs) of the viral vector (white boxes) are indicated. SA and SD are the splicing acceptor site and donor site, respectively; neo^r, neomycin resistance gene. (B) *Mdm4* wild-type and mutant embryos (homozygous) at different stages of embryonic development (E10.5 and E11.5). (C) *Mdm4*/*Trp53* wild-type and mutant (heterozygous and homozygous) embryos at different stages of embryonic development (E10.5 and E12.5). (D) PCR analysis of embryos with the indicated genotypes. The positions of the three primers a, b, and c are indicated. (E) Western blotting analysis of Mdm4 protein expression. NIH 3T3 cells (as a control) or mouse brain protein extracts from wild-type (*Mdm4*$^{+/+}$ *Trp53*$^{+/+}$) or mutant (*Mdm4*$^{+/-}$ *Trp53*$^{+/+}$, *Mdm4*$^{+/-}$ *Trp53*$^{+/-}$, and *Mdm4*$^{-/-}$ *Trp53*$^{-/-}$) embryos were immunoprecipitated with the anti-Mdm4 rabbit polyclonal antibodies p55, p56, and SI23 (anti-X [α-X]) or with preimmune (PI) serum. Mdm4 was detected by Western blot analysis using a mixture of monoclonal antibodies 6B1A and 11F4D.

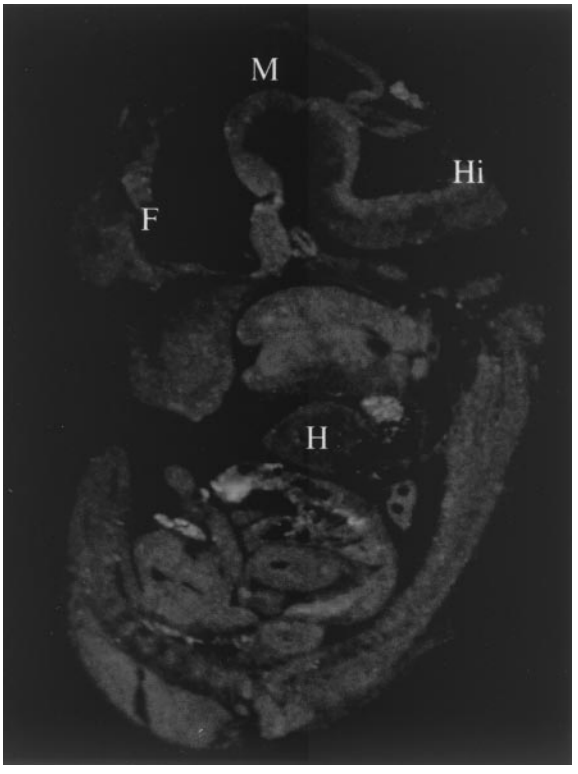

FIG. 2. ISH analysis of an E11.5 mouse embryo with an Mdm4 antisense probe. Abbreviations: F, forebrain; M, midbrain; Hi, hindbrain; H, heart.

To examine the relative plating efficiencies, passage 3 MEFs were plated at 1×10^3, 2×10^3, and 4×10^3 cells per plate onto 10-cm-diameter plates, cultured for about 10 days, and then washed twice with PBS, fixed, and stained for 5 min (1% crystal violet in 35% methanol). Colonies containing >50 cells were counted.

To compare the survival of the various genotypes, MEFs following treatment with DNA-damaging agents, duplicate plates of two different lines of wild-type, *Trp53*$^{-/-}$ *Mdm4*$^{+/+}$, *Trp53*$^{-/-}$ *Mdm4*$^{+/-}$, or *Trp53*$^{-/-}$ *Mdm4*$^{-/-}$ cells were plated onto 10-cm-diameter dishes at low density (10^4 cells per plate). Twenty-four hours after the cells were plated, they were exposed to increasing UV radiation with a UV stratalinker (Stratagene). Ten days after exposure, the cells were fixed and stained for 5 min (1% crystal violet in 35% methanol). Colonies containing >50 cells were counted.

Cell cycle studies. For analysis of the *Mdm4*$^{-/-}$ cells, 10^5 cells were seeded 24 h on glass coverslips in 12-well dishes prior to treatment to prevent contact inhibition. The cultures were pulse-labeled with 10 μM BrdU (Sigma) for 1 h, the coverslips were then fixed for10 min in 4% paraformaldhehyde–1× PBS. For the G_1/S cell cycle progression assay, cells were synchronized at G_0 by culturing in medium supplemented with 0.1% FBS for 96 h. Cells were then trypsinized and seeded on glass coverslips at a low density in 12-well dishes (2.5×10^4 cells per well) in normal growth medium supplemented with 10 μM BrdU (Sigma). After 24 h of BrdU labeling, cells were fixed 10 min in 4% paraformaldhehyde–1× PBS. The BrdU-positive cells were identified by indirect immunofluorescence essentially as described above, except that the primary antibody (anti-BrdU mouse monoclonal antibody; Sigma) was diluted in blocking buffer containing 3 mM $MgCl_2$ plus 100 U of DNase I (Boehringer) per ml. The secondary antibody was a fluorescein isothiocyanate-conjugated anti-mouse antibody.

For the cell cycle analysis of the double p53/Mdm4-deficient cells, 1.2×10^6 MEFs, passage 3, were plated onto 10-cm-diameter dishes 24 h prior treatment. Cultures were either left untreated or treated with 8 Gy of gamma irradiation (^{137}Cs source at a rate of 0.86 Gy/min). After 48 h, the cultures were pulse-labeled with 10 μM BrdU for 1 h, harvested by trypsinization, and fixed in 70% ethanol. Alternatively, cells were synchronized at G_0 by culturing in medium supplemented with 0.1% FBS for 96 h. MEFs were either untreated or treated with 8 Gy of gamma irradiation, cultured for 24 h in normal growth medium supplemented with 10 μM BrdU (Sigma), harvested by trypsinization, and fixed in 70% ethanol. DNA synthesis and DNA content were analyzed by flow cytometry as previously described (12). In brief, BrdU-labeled cells fixed in 70% ethanol were treated with 2 N HCl (20 min at room temperature [RT]) followed by addition of 2 volumes of 0.1 M sodium borate (pH 8.5). The cells were incubated (1 h at RT) with an anti-BrdU mouse monoclonal antibody, washed, and incubated (1 h at RT) with fluorescein isothiocyanate-conjugated anti-mouse antibody. Cells were counterstained overnight with 5 μg of propidium iodide per ml containing 40 μg of RNase per ml. The stained cells were analyzed with a FACscan (Becton-Dickinson) using a cellQuest program.

TABLE 2. Genotypes of mice from *Mdm4*$^{+/-}$ *p53*$^{+/-}$ × *Mdm4*$^{+/-}$ *p53*$^{+/-}$ crosses

Genotype	No. of mice			Total no. of mice
	Mdm4$^{+/+}$	*Mdmx*$^{+/-}$	*Mdmx*$^{-/-}$	
p53$^{+/+}$	7	26	0	33
p53$^{+/-}$	17	22	0	39
p53$^{-/-}$	7	16	7	30
Total	31	64	7	102

RESULTS

A gene trap event in the *Mdm4* locus leads to a *Mdm4*-null phenotype and causes a p53-dependent embryonic lethality. An ES cell clone with a specific gene trap event in the *Mdm4* locus was microinjected into host blastocysts to produce a *Mdm4* gene trap mouse line (38). The insertion gene trap vector, based on Moloney murine leukemia virus, had integrated into an intron, between exons 1 and 2 (Fig. 1A). Heterozygous mice for this mutation were viable and fertile. However, matings between heterozygous animals produced no viable homozygous mutant offspring, indicating a recessive lethal phenotype (Table 1 and Fig. 1D for a representative genotype assay).

Closer inspection revealed that most homozygous embryos (*Mdm4*$^{-/-}$) died in utero between 9.5 and 11.5 days postcoitum (dpc). The majority of the E9.5 *Mdm4* mutants and 100% of the E10.5 *Mdm4* mutants exhibited an overall growth deficiency, ranging from minor to extremely severe, and a head developmental defect, characterized by improper neural tube closure and dilation of the lateral ventricles (Fig. 1B). The growth defect was not due to a developmental arrest, since *Mdm4*$^{-/-}$ mutants displayed developmental features characteristic of their embryonic age. In addition to these defects, all E11.5 *Mdm4* mutant embryos were strikingly paler than the control embryos, indicative of failed fetal liver hematopoiesis. No viable mutants were observed beyond E12.5 (Table 1). At E13.5, most of the *Mdm4*$^{+/-}$ embryos were slightly smaller and paler than wild-type littermates, suggesting that even haploid loss of *Mdm4* compromises normal embryonic development (not shown). Consistent with an overall impact of the mutation throughout the whole embryo at 11.5 dpc, *Mdm4* was ubiquitously expressed at this developmental stage, as demonstrated by ISH experiments (Fig. 2).

Since Mdm4 has been shown to inhibit p53 transcriptional ability in vitro (11, 18, 31–33), we tested whether loss of the *Trp53* gene affected the survival of *Mdm4* mutant embryos by transferring the *Mdm4* mutation into a *Trp53*-null background (10). Strikingly, loss of both Trp53 alleles completely abro-

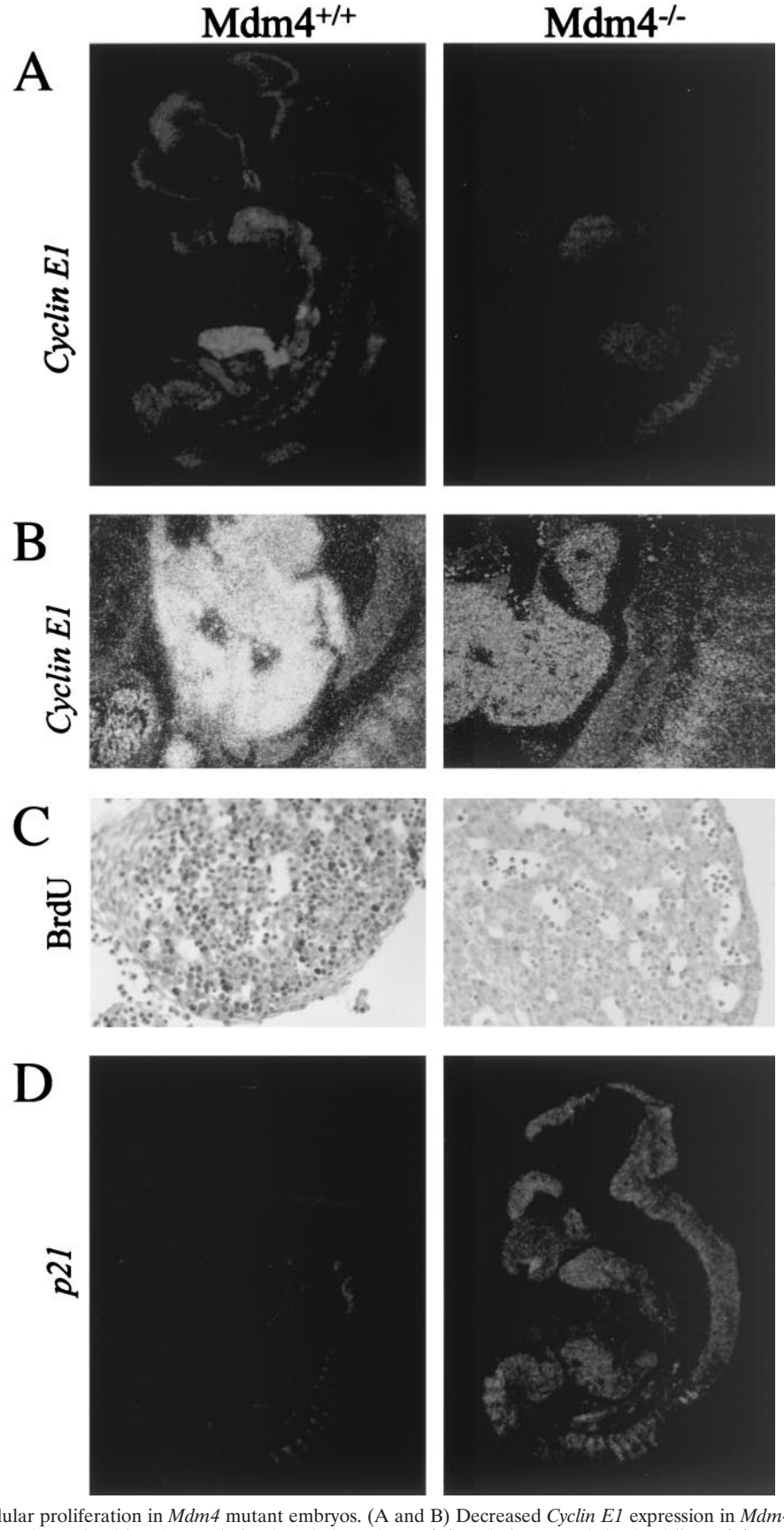

FIG. 3. Impaired cellular proliferation in *Mdm4* mutant embryos. (A and B) Decreased *Cyclin E1* expression in $Mdm4^{-/-}$ embryos compared to wild-type littermates as determined by ISH analysis; the whole embryos (A) and close-up of the fetal livers (B) are shown. (C) Analysis of proliferation of the fetal liver hematopoietic progenitors. Embryos were stained with an antibody to detect in vivo BrdU incorporation and counterstained using hematoxylin and eosin. Very few BrdU-positive cells are found in the fetal liver of *Mdm4* homozygous mutant embryos. (D) Increased *p21* expression in $Mdm4^{-/-}$ embryos compared to wild-type littermates as determined by ISH analysis.

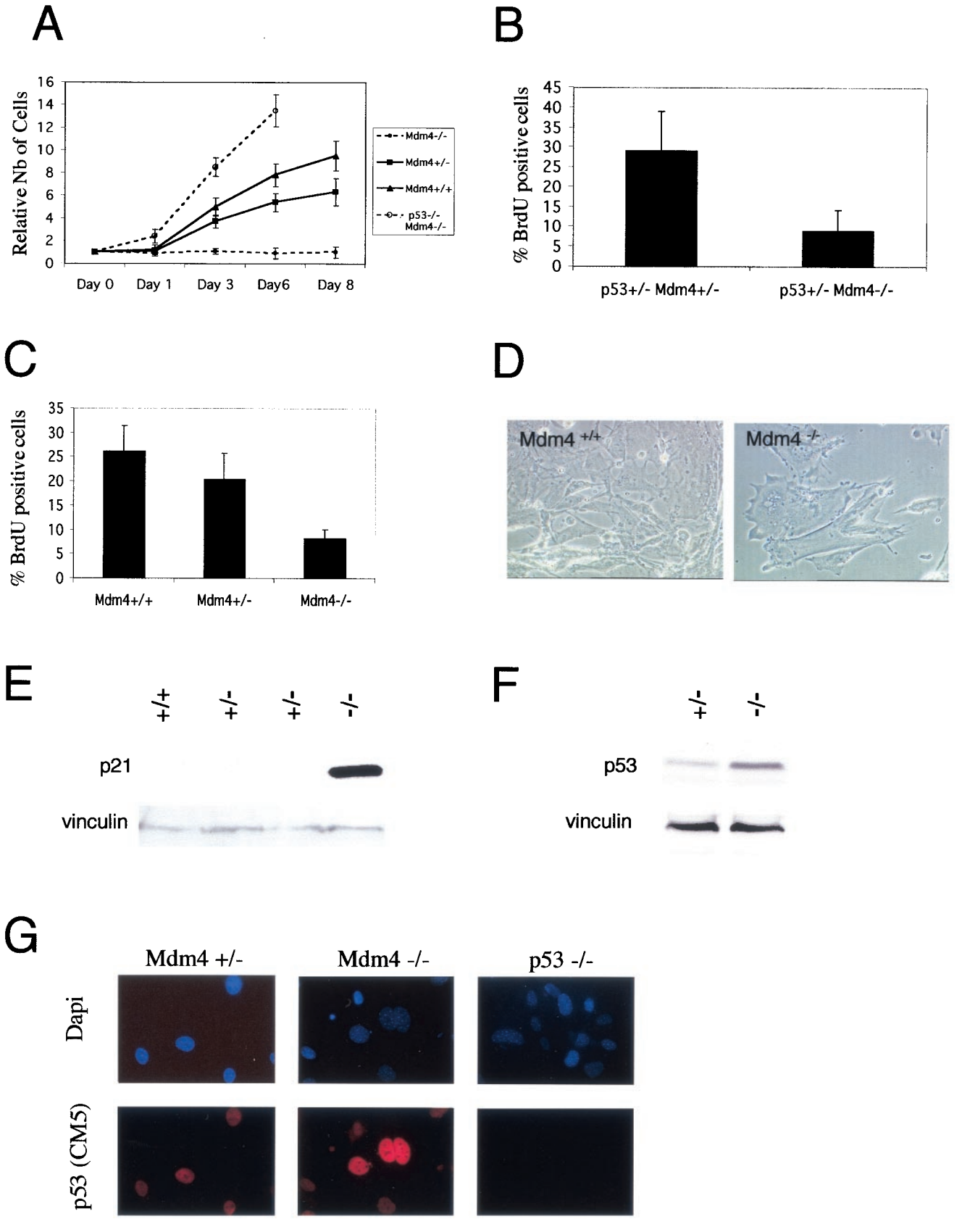

FIG. 4. (A to D) Impaired proliferation of *Mdm4*-null fibroblasts in cultures. (A) Growth curves for $Mdm4^{+/+}$, $Mdm4^{+/-}$, $Mdm4^{-/-}$, and $Mdm4^{-/-}$ $Trp53^{-/-}$ MEF cultures at passage 2. A total of 2.5×10^4 cells were plated into 12-well plates. Cultures were harvested at daily intervals,

gated the effect of the *Mdm4* mutation. *Mdm4*$^{-/-}$ *Trp53*$^{-/-}$ viable and healthy mice were obtained at the expected Mendelian ratio (1/16; of 102 mice born from such crosses, 7 were *Trp53*$^{-/-}$ *Mdm4*$^{-/-}$) (Table 2), and *Mdm4*$^{-/-}$ *Trp53*$^{-/-}$ embryos appeared morphologically undistinguishable from wild-type embryos, as shown here at E10.5 of embryonic development (Fig. 1C). Although, no viable *Mdm4*$^{-/-}$ *Trp53*$^{+/-}$ mouse could be found from double heterozygous intercrosses, even haploid loss of *Trp53* significantly reduced the effect of the *Mdm4* mutation (Fig. 1C).

Finally, to investigate whether Mdm4 was produced, we analyzed the levels of Mdm4 protein in total brain protein extracts from *Trp53*$^{+/+}$ *Mdm4*$^{+/+}$, *Trp53*$^{+/+}$ *Mdm4*$^{+/-}$, *Trp53*$^{+/-}$ *Mdm4*$^{+/-}$, and *Trp53*$^{-/-}$ *Mdm4*$^{-/-}$ adult mice. Mdm4 was absent from *Trp53*$^{-/-}$ *Mdm4*$^{-/-}$ extracts and present at about half normal levels in *Mdm4*$^{+/-}$ extracts, irrespective of the *Trp53* genotype (Fig. 1E). A combination of antibodies which recognizes different Mdm4 epitopes was used to ensure detection of all possible Mdm4 protein variants (see Materials and Methods). These results show that, as opposed to the previously reported *Mdm4* mouse mutant (25), which retained expression of a short Mdm4 product, this is a null Mdm4 mutation.

Failure in cell proliferation in *Mdm4* mutants. To study the effect of the *Mdm4* mutation on cellular proliferation, we measured in situ incorporation of BrdU and expression levels of *Cyclin E1* and proliferating cell nuclear antigen by ISH or immunohistochemistry, respectively. For each of these proliferation markers, signal was markedly reduced in the whole *Mdm4* mutant embryos (shown for *Cyclin E1* in Fig. 3A and B). This was particularly notable around E12 in the fetal liver, a site of intense cell proliferation due to the massive expansion of committed erythroid lineage cells (shown for *Cyclin E1* and BrdU incorporation in Fig. 3). Together, these results suggest a generalized failure in cell proliferation in the *Mdm4* mutants, thus providing an explanation for the reduced size and the paleness of the *Mdm4* mutant embryos.

The reduced incorporation of BrdU, which directly measures S-phase cells, suggests a defect in the G_1/S transition of the mutant embryos. This is consistent with the observed reduced levels of *Cyclin E1*, whose expression peaks at the G_1/S transition (15) and controls S-phase entry (22, 23). Therefore, we analyzed the in situ expression of *p21*$^{CIP1/Waf1}$, a well-known p53 target gene, encoding a potent CDK inhibitor that mediates the p53-dependent G_1-S cell cycle checkpoint (4, 6). All mutant embryos showed an overall and dramatic increased expression of *p21*, as demonstrated by ISH (Fig. 3D). Real-time quantitative reverse transcription-PCR assay (not shown) and Western blotting analysis (Fig. 4E) confirmed the strong up-regulation of p21 (up to 10-fold in some *Mdm4* mutant embryos). It appears, therefore, that *Mdm4* mutant embryos accumulate cells blocked at the G_0-G1 phase of the cell cycle.

***Mdm4*-deficient fibroblasts exhibit a p53-dependent reduced proliferative capacity.** To characterize the role of Mdm4 in the regulation of p53 activity, we investigated the effect of *Mdm4* deficiency on the life span of explanted MEFs. MEFs, in fact, undergo 10 to 12 population doublings in culture, after which, as a consequence of a p53-dependent cell cycle checkpoint, they cease division and develop a so-called senescent phenotype.

E10.5 *Mdm4*$^{-/-}$ MEFs showed a dramatic reduction of their proliferation rate compared to *Mdm4*$^{+/+}$ cells, whereas MEFs from heterozygous embryos had an intermediate behavior (Fig. 4A). BrdU incorporation experiments showed a marked reduction of cycling cells in the *Mdm4*$^{-/-}$ cells, suggesting an S-phase defect (see Fig. 4B for BrdU incorporation values of *Trp53*$^{+/-}$ *Mdm4*$^{+/-}$ and *Trp53*$^{+/-}$ *Mdm4*$^{-/-}$ MEFs). Cultured *Mdm4*$^{-/-}$ MEFs showed morphological (cytoplasmic enlargement and flattening of the cells [Fig. 4D]) and functional (unresponsiveness to growth factors [Fig. 4C]) properties of premature senescence, as early as after two passages of culture. The reduced proliferation potential of *Mdm4*$^{-/-}$ MEFs was entirely p53 dependent, since it was completely rescued in the absence of p53 (Fig. 4A). Cells lacking both Mdm4 and p53 proliferated even faster than wild-type cells (*Mdm4*$^{+/+}$) (Fig. 4A), to an extent comparable with p53-null cells (Fig. 5A).

We next investigated the levels of p53 in the *Mdm4*$^{-/-}$ background and controls. Western blotting (Fig. 4F) and indirect immunofluorescence (Fig. 4G) analyses revealed that loss of Mdm4 expression is associated with a significant increase in basal p53 protein levels. Accordingly, and in agreement with our ISH data (Fig. 3D), Western blotting analysis revealed markedly higher levels of p21 protein expression in passage 1 *Mdm4*$^{-/-}$ MEFs than in matched controls (Fig. 4E). Together, these data clearly indicate that the ability of the *Mdm4*-null fibroblasts to prematurely lose their proliferative capacity is a direct consequence of constitutive p53 activation.

No critical role for Mdm4 in cell proliferation and cell cycle control independently of p53. To determine whether Mdm4 can modulate cell cycling in a p53-independent manner, we examined a number of in vitro growth properties of p53- and *Mdm4*/*Trp53*-deficient MEFs. For each experiment, we used passage 3 fibroblasts from two separate lines of each genotype.

MEFs were prepared and counted at various time points

and the total number of cells were determined and normalized to the number of cells at day 0 (20 h after plating) (relative number [Nb] of cells). The numbers refer to the mean values of two independently derived MEF cultures of each genotype. (B) Level of BrdU incorporation by asynchronously growing passage 2 *Mdm4*$^{+/-}$ *Trp53*$^{+/-}$ and *Mdm4*$^{-/-}$ *Trp53*$^{+/-}$ MEFs. (C) Quantitative analysis of the percentage of S-phase cells after serum stimulation for 24 h of G_0-synchronized *Mdm4*$^{+/+}$, *Mdm4*$^{+/-}$, and *Mdm4*$^{-/-}$ MEF cultures. The BrdU-labeled MEFs were analyzed by indirect immunofluorescence, and the S-phase cells were determined by staining with anti-BrdU antibody. (D) Photomicrographs of MEFs at passage 2. *Mdm4*-null MEFs were growth arrested; *Mdm4*$^{+/+}$ MEFs were not growth arrested. (E) Constitutive high levels of p21 protein expression in *Mdm4*$^{-/-}$ MEFs at passage 1. Western blotting analysis from *Mdm4*$^{+/+}$ cell lysates, two independent *Mdm4*$^{+/-}$, and *Mdm4*$^{-/-}$ MEF cultures at passage 1. Vinculin serves as loading control. (F and G) Constitutive high levels of p53 protein expression in *Mdm4*$^{-/-}$ MEFs at passage 3. (F) p53 protein levels determined by Western blotting analysis using the sheep polyclonal antibody Ab-7 from *Mdm4*$^{+/-}$ and *Mdm4*$^{-/-}$ MEF cell lysates. Vinculin serves as a loading control. (G) p53 protein (red) levels examined by indirect immunofluorescence using the rabbit polyclonal antibody CM5 in *Mdm4*$^{+/-}$ and *Mdm4*$^{-/-}$ MEF cultures. The DNA (blue) is stained with 4′,6′-diamidino-2-phenylindole (Dapi). The absence of signal in *Mdm4*$^{+/-}$ *Trp53*$^{-/-}$ MEF cultures demonstrates the specificity of the antibody.

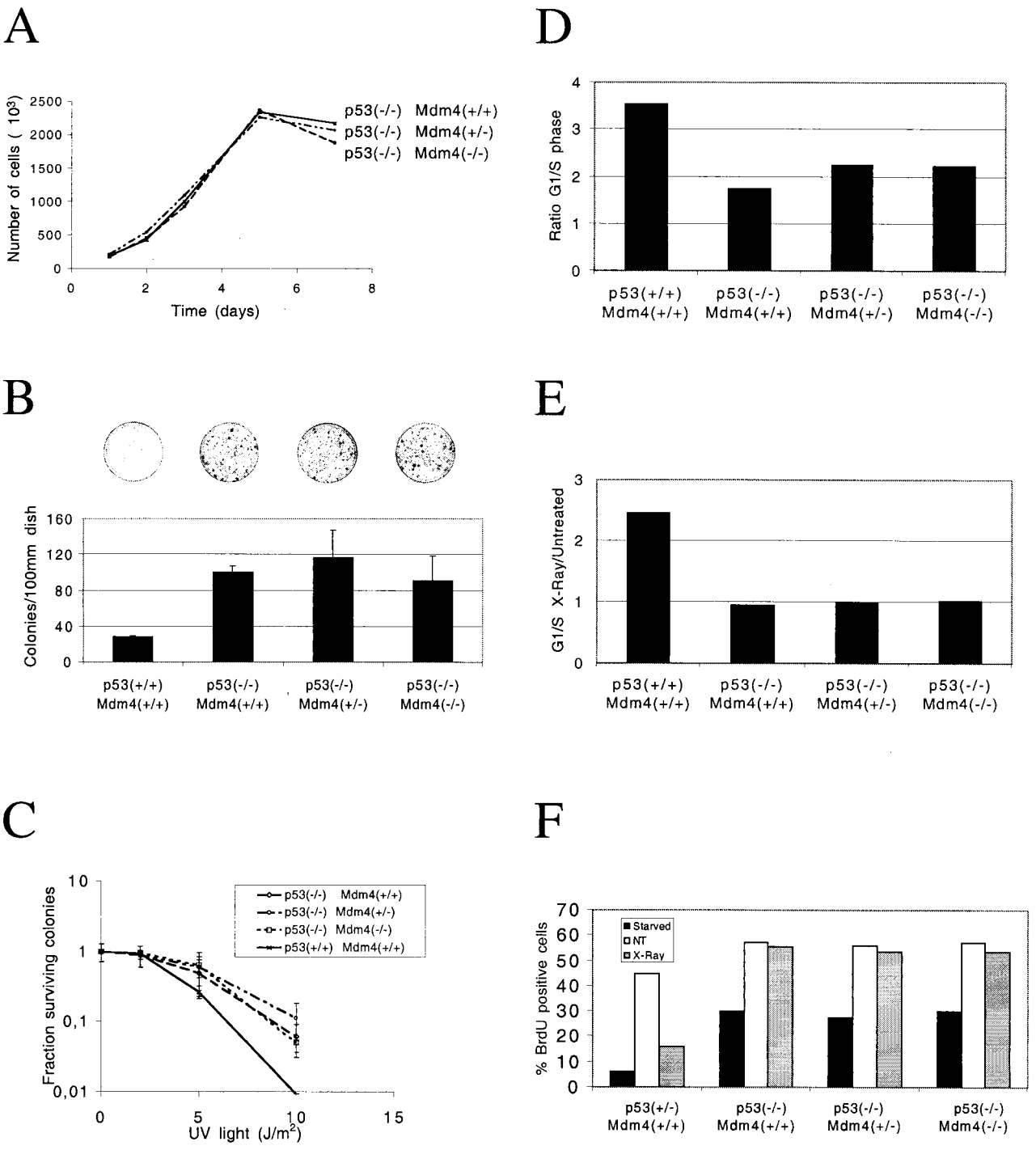

FIG. 5. (A and B) Proliferation of embryonic fibroblasts (A) Growth rates of fibroblasts that are either wild type, heterozygous, or nullizygous for Mdm4 and nullizygous for p53. Cell numbers at each point represent an average of two separate lines of cells, two plates of cells for each line. (B) Colony formation of wild-type, heterozygous, or nullizygous for Mdm4 and p53 MEFs grown in conditions of low cell density (10^3 cells per 10-cm-diameter plate). Values given represent an average of two plates each of two lines of cells. Bars indicating standard deviation values are shown. A total of 2×10^3 cells were plated (10-cm-diameter dishes), cultured, fixed, and stained. Representative dishes are shown over the bars for the corresponding genotypes. (C) Colony formation following DNA damage. Wild-type MEFs or MEFs heterozygous or nullizygous for Mdm4 and p53 were plated at low density (10^4 cells per 10-cm-diameter dish) following treatment with increasing UV irradiation (2, 5, and 10 J/m^2). Two independent experiments were performed, and the mean values with standard deviations (error bars) are presented. (D, E, and F) Cell cycle analysis on embryonic fibroblasts determined by FACScan analysis. The S-phase cells (BrdU-positive cells) are revealed by staining with anti-BrdU antibody, and DNA content is revealed with propidium iodide. (D) G_1/S ratio of MEFs that are wild type, heterozygous, or nullizygous for Mdm4 and p53. (E) Effects of gamma irradiation on the cell cycles of MEFs that are wild type, heterozygous, or nullizygous for Mdm4 and p53. The G_1/S ratio is given compared to untreated G_1/S values. (F) S-phase entry following serum stimulation and gamma irradiation of synchronized MEFs that are wild type, heterozygous, or nullizygous for Mdm4 and p53. The percentages of cells in the S phase of the cell cycle immediately after starvation, cells grown for 24 h in growth medium (not treated [NT]), or cells that had undergone gamma irradiation (X-Ray).

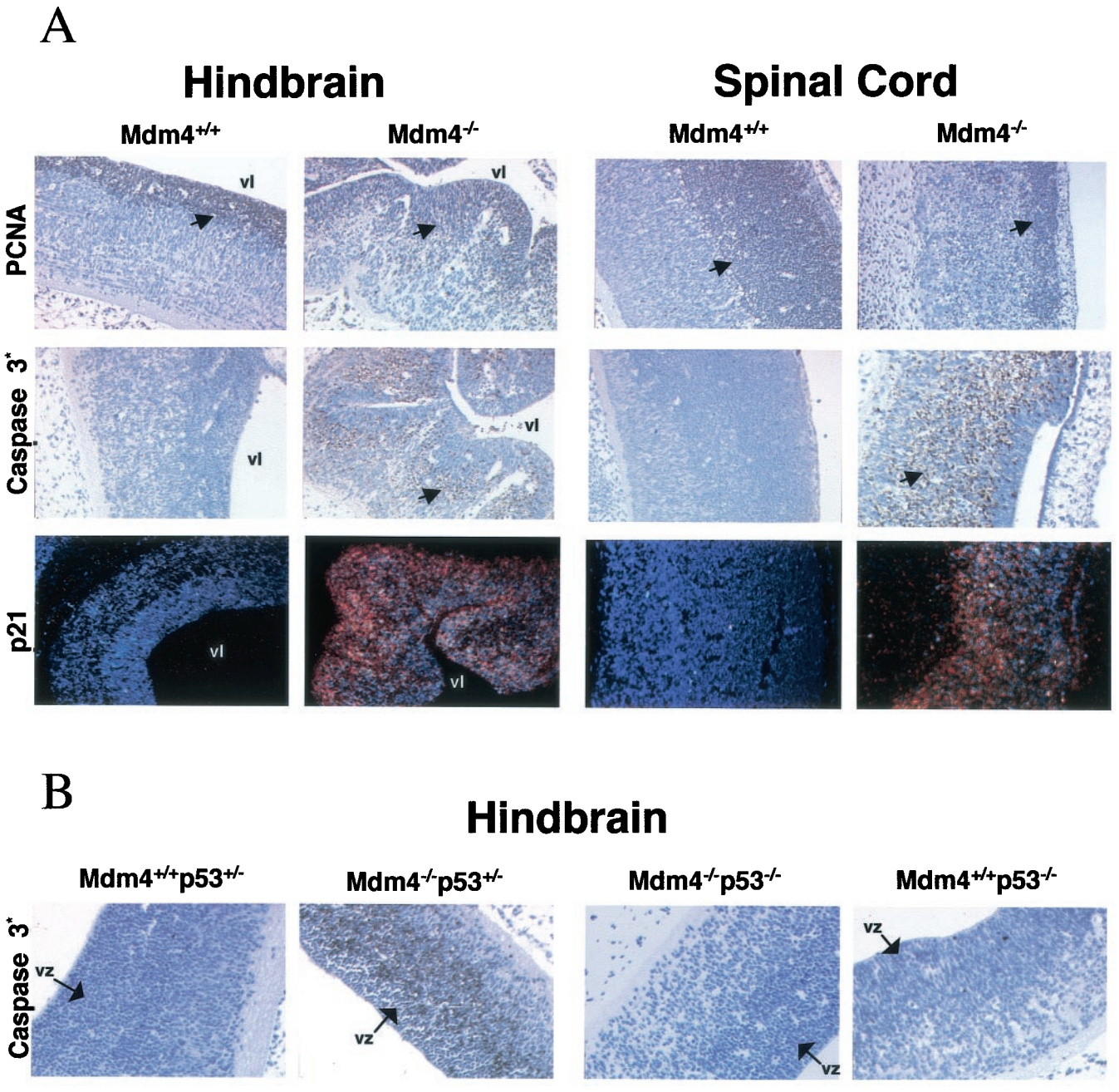

FIG. 6. (A) Analysis of proliferation, apoptosis, and p21 expression levels in the developing CNS (hindbrain and spinal cord) of *Mdm4*$^{-/-}$ and *Mdm4*$^{+/+}$ embryos 12 days postcoitum. We stained wild-type and *Mdm4* mutant embryos with antibody recognizing PCNA to detect cell proliferation and with antibody directed against the activated form of caspase 3 to detect apoptosis. The *p21* expression pattern in the same regions of the CNS was determined by ISH. Dark field (red signal) view of sections counterstained with Hoechst (blue signal). Positive cells are indicated by the arrows. vl, ventricular lumen. (B) Absence of apoptosis in the developing CNS of E11.5 *Mdm4*$^{-/-}$ *p53*$^{-/-}$ embryos. *Mdm4*$^{+/+}$ *p53*$^{+/-}$, *Mdm4*$^{-/-}$ *p53*$^{+/-}$, *Mdm4*$^{-/-}$ *p53*$^{-/-}$, and *Mdm4*$^{+/+}$ *p53*$^{-/-}$ embryos were stained with antibody directed against the activated form of caspase 3 to detect apoptosis. The ventricular zone (vz) is indicated.

following initial plating. As expected, *Trp53*$^{-/-}$ fibroblasts have a higher rate of cell proliferation than *Trp53*$^{+/-}$ or *Trp53*$^{+/+}$ fibroblasts (not shown) (9). There was, however, no significant difference in the proliferative rates or saturation densities of *Trp53*$^{-/-}$ *Mdm4*$^{+/+}$ fibroblasts and *Trp53*$^{-/-}$ *Mdm4*$^{+/-}$ or *Trp53*$^{-/-}$ *Mdm4*$^{-/-}$ fibroblasts (Fig. 5A).

We then investigated the ability of MEFs to survive and proliferate when plated at very low densities (colony formation at clonal densities) (Fig. 5B). As previously reported, 10 times more colonies were present on plates seeded with p53-deficient cells compared to wild-type cells (13). However, no significant difference was detected for *Trp53*$^{-/-}$ fibroblasts that were wild type, heterozygous, or nullizygous for functional Mdm4.

Cells were then plated at low densities and treated with

increasing doses of UV, and colonies were counted 10 days after treatment (UV radiation survival assay; Fig. 5C). As previously reported for the *Trp53*$^{-/-}$ MEFs (13), this treatment led to decreased survival of cells from all four genotypes. Although a difference in the survival of wild-type and p53-deficient cells was particularly evident at higher dose points, no difference was detected in the survival of p53-deficient cells and cells deficient for both p53 and Mdm4 at any dose.

To unravel a putative role of Mdm4 in promoting cell cycle progression independently of p53, MEFs were pulsed with BrdU for 1 h and the numbers of cells present in the G_1 and S phases of the cell cycle were determined using flow microfluorometry analysis (Fig. 5D). As expected, the G_1/S ratio of p53-deficient cells was decreased relative to wild-type cells (9). However, there was no difference in the G_1/S ratio of *Trp53*$^{-/-}$ *Mdm4*$^{+/+}$, *Trp53*$^{-/-}$ *Mdm4*$^{+/-}$, and *Trp53*$^{-/-}$ *Mdm4*$^{-/-}$ fibroblasts.

Cells were then gamma irradiated (8 Gy), and the ratio of cells in the G_1 and S phases of the cell cycle were compared with untreated G_1/S ratio values (Fig. 5E). Irradiation of wild-type cells, but not p53-deficient cells, resulted in increased relative number of G_1 cells, consistent with the notion that p53 is required to block progression of cells into S phase following DNA damage. Irradiated *Trp53*$^{-/-}$ *Mdm4*$^{+/-}$ and *Trp53*$^{-/-}$ *Mdm4*$^{-/-}$ fibroblasts exhibited the same G_1/S phase ratio as the p53-deficient cells. In the same lines, MEFs synchronized at G_0 by serum starvation were treated with 0 or 10 Gy of gamma irradiation, released into serum-containing medium, and evaluated for BrdU incorporation (Fig. 5F). Irrespective of the presence of functional Mdm4, the percentages of BrdU-positive cells were comparable for all p53-deficient cells, while there was more than 50% reduction of S-phase cells in wild-type MEFs following gamma irradiation. Together these data suggest that Mdm4 does not affect the ability to enter S phase following DNA damage through a p53-independent pathway.

Finally, to determine whether the absence of Mdm4 affects the rate of spontaneous immortalization of p53-deficient cells, MEFs were passaged in culture following the classical 3T3 protocol. Once again, no difference was observed in growth properties of the various cell lines, suggesting that the absence of Mdm4 does not alter the induction of immortality in p53-deficient cells during long-term passage in culture (not shown).

Spontaneous apoptosis in the CNS of *Mdm4* mutants. To determine if the growth deficit of *Mdm4* mutant embryos could also be accounted by an excess of apoptosis, serially sectioned E9.5 to E11.5 embryos were analyzed by immunohistochemistry using an antibody specific to the cleaved form of caspase 3 (21). This analysis revealed extensive cell death in the developing CNS, particularly evident at the latest stages of embryonic development (E11.5) (Fig. 6A). Interestingly, this phenotype was specific to neural tissue, not being found in any other cell types of the mutant embryos (not shown), and directly p53 dependent, since it was not detected in the *Trp53*$^{-/-}$ *Mdm4*$^{-/-}$ brain (Fig. 6B). As a consequence of cell death, the telencephalic wall was thinner and lateral ventricles were larger than those of the control. Closer inspection of the hindbrain and spinal cord neuroepithelium revealed apoptosis predominantly in cells of the mantle (or intermediate) zone, while the PCNA-positive, highly proliferating, neuronal precursor cells of the ventricular zone appeared largely protected (Fig. 6A). Although reduced in numbers, these PCNA-positive neuroblasts were present in the *Mdm4* mutant embryos. They also appeared mainly *p21* negative by ISH (Fig. 6A), suggesting that p53 function is tightly regulated in these cells.

DISCUSSION

Our findings demonstrate that Mdm4, like Mdm2, plays an indispensable and nonredundant role in the suppression of p53 basal activity during mouse embryonic development. Analysis of another *Mdm4* mouse mutant has recently led to similar conclusions (25). However, in that study, interpretation of results is complicated by the expression of a short hypomorphic *Mdm4* product, with putative dominant negative activity towards Mdm2. The partial inhibition of Mdm2 function might, indeed, explain the remarkable differences of the two *Mdm4* mutants, e.g., the severity of the phenotypes and the different biological consequences of p53 activation. Mdm2 deficiency resulted in lethality right after implantation (E5.5) (12, 20). The *Mdm4* mutant embryos described by Parant et al. (25) do not develop after E7.5, while the *Mdm4*-null mutation reported here leads to an embryonic lethality around 10.5 to 11.5 dpc. The previously reported *Mdm4* mutants showed loss of cell proliferation and not induction of apoptosis, suggesting that Mdm4 is able to regulate only one aspect of p53 function, namely, control of cell growth. We observed, instead, either p53-dependent cell growth arrest or extensive cell death, depending on the cell type.

Absence of Mdm4 expression leads to increased p53 protein stability and, although not formally demonstrated here biochemically, to p53 constitutive activation. As a consequence, one of the p53-responsive genes, *p21*$^{CIP1/WAF1}$, was found dramatically and quasi ubiquitously up-regulated in our *Mdm4*-deficient embryos. Since p21 is involved in the inhibition of G_1-to-S-phase cell cycle progression, this may account for the growth defect observed in the *Mdm4* mutant embryos. Similarly, increased p21 protein levels in *Mdm4*-deficient cells (MEFs) could account for their proliferative defects, including slower proliferation, inefficient cell cycle G_1/S progression and unresponsiveness to growth factors. We are currently testing this possibility by transferring the *Mdm4* mutation into a *p21*-null background.

However, why some cells undergo cell cycle arrest (fetal liver hematopoietic cells, for instance) and others show a p53 apoptotic response (neuronal cells) remains unanswered (for a review, see reference 36). One possible explanation is that the profile of genes transcriptionally regulated by p53 differs in different cell populations or under different physiological conditions, such as growth. This mouse model may then provide a useful tool for the identification of modulators and/or effectors of the cell fate following p53 activation. It would, for instance, be of interest to study in greater detail the expression pattern of newly identified p53-responsive genes or new putative p53 regulators such as the ASPP proteins in *Mdm4*-deficient embryos (28).

Regardless of molecular mechanisms, the consequences of massive apoptosis in the *Mdm4*-null embryos are dramatic for brain development, confirming that tight regulation of p53 is essential for neural development (for reviews, see references 8 and 19). The brain mantle of *Mdm4*-deficient embryos was

thinner and the lateral ventricles were larger than in control embryos, and readily apparent hydrocephalus was frequently found. Notably, this phenotype is reminiscent of that reported for mice treated with X-rays at early gestational stages (2). In wild-type embryos, p53 protein is detectable only in the developing nervous system (8 and 10 days postcoitum), in particular in the mantle layer of the spinal cord, and the observed protein is transcriptionally active (17). Additional evidence supporting a role for p53 in neural progenitor cell development came from studies of mice lacking the pRb tumor suppressor protein which demonstrated the existence, in neural precursors, of an intrinsic p53-dependent apoptotic pathway involved in the elimination of cells that fail to differentiate properly (for a review, see reference 19). In addition, activation of the p53 protein following ionizing irradiation results in marked neuronal cell death (17). Similarly, lack of Mdm4 expression, as in our mutant mice, results in constitutive p53 activation and extensive p53-dependent apoptosis in the CNS.

The data in this report strongly indicate that the predominant role of Mdm4, as proposed for Mdm2 earlier (13), is to inactivate p53 function. First, the absence of p53 rescues the embryonic lethal phenotype of Mdm4-deficient mice and the double nullizygous Mdm4/p53 mice are viable. This observation indicates that any non-p53-mediated functions possessed by Mdm4 are not critical for embryonic development and survival. Second, we did not observe any differences in the rate of proliferation, immortalization frequency, survival after genotoxic insult, or cycling of cells that were deficient for p53 or both p53 and Mdm4. We are currently analyzing the rate and the spectrum of tumor formation in p53-deficient and Mdm4/p53-deficient mice. However, based on the results presented here, one might expect these mice to exhibit similar incidence and spectrum of spontaneous tumor formation in vivo.

A recent report has documented the ability of Mdm4 to inhibit the transcriptional activity of ectopically expressed SMAD proteins (SMAD1, SMAD2, SMAD3, and SMAD4) (37). These proteins play a key role in the transforming growth factor β signal transduction pathway and have therefore been implicated in the control of cell proliferation in many cell types. Moreover, Mdm4 has been implicated in the regulation of the transcriptional activity of the p53-related protein, p63 (14) and interaction between p73α and Mdm4 has also been reported (24). Based on our observations, it is difficult to envision a critical role for Mdm4 in the regulation of the activity of these transcription factors. However, since Mdm2 has also been shown to negatively regulate the same factors, it is possible that, in contrast to the regulation of p53, Mdm2 and Mdm4 regulate the transcriptional abilities of these proteins in a redundant manner. We are currently testing this possibility by generating mice that lack functional p53 and both Mdm2 and Mdm4. Alternatively, Mdm4 may only interfere with the activities of these proteins upon overexpression.

Finally, one of the major implications of this work is that Mdm4, like Mdm2, is a critical negative regulator of p53 function in vivo, thereby suggesting a role for Mdm4 in tumorigenesis. Hdm2 is frequently amplified and/or overexpressed in a number of human tumors, many of which lack mutations in *Trp53* (for a review, see reference 5). Interestingly, increased Hdm4 levels were found in a significant fraction of tumor cell lines, and in general, Hdm4 expression in these cells correlates with the presence of wild-type p53 (26). Moreover, we have recently obtained preliminary evidence suggesting that increased Mdm4 levels cause inactivation of p53 function in tissue culture. It will be, therefore, of interest to determine whether Hdmx overexpression occurs in human neoplastic cells.

ACKNOWLEDGMENTS

Domenico Migliorini, Eros Lazzerini Denchi, and Davide Danovi contributed equally to this work.

We thank S. Minucci and M. Faretta for many helpful discussions and/or critically reviewing this manuscript.

This work was supported in part by grants from AIRC and EC. J.-C. Marine is a recipient of a fellowship from European Community (Marie Curie Fellowship). E.L.D. is a recipient of a fellowship from The FIRC Institute of Molecular Oncology.

REFERENCES

1. **Angerer, L. M., and R. C. Angerer.** 1991. Localizations of mRNAs by *in situ* hybridisation. Methods Cell Biol. **35:**37–71.
2. **Aolad, H. M., M. Inouye, W. Darmanto, S. Hayasaka, and Y. Marata.** 2000. Hydrocephalus in mice following X-irradiation at early gestational stage, possibly due to persistent deceleration of cell proliferation. J. Radiat. Res. **41:**213–226.
3. **Boyd, S. D., K. Y. Tsai, and T. Jacks.** 2000. An intact HDM2 RING-finger domain is required for nuclear exclusion of p53. Nat. Cell Biol. **2:**563–568.
4. **Brugarolas, J., C. Chandrasekaran, J. I. Gordon, D. Beach, T. Jacks, and G. J. Hannon.** 1995. Radiation-induced cell cycle arrest compromised by p21 deficiency. Nature **377:**552–557.
5. **Daujat, S., H. Neel, and J. Piette.** 2001. MDM2: life without p53. Trends Genet. **17:**459–464.
6. **Deng, C., P. Zhang, J. W. Harper, S. J. Elledge, and P. Leder.** 1995. Mice lacking p21CIP1/WAF1 undergo normal development, but are defective in G1 checkpoint control. Cell **82:**675–684.
7. **Geyer, R. K., Z. K. Yu, and C. G. Maki.** 2000. The MDM2 RING-finger domain is required to promote p53 nuclear export. Nat. Cell Biol. **2:**569–573.
8. **Hall, P. A., and D. P. Lane.** 1997. Tumour suppressors: a developing role for p53? Curr. Biol. **7:**144–147.
9. **Harvey, M., A. T. Sands, R. S. Weiss, M. E. Hegi, R. W. Wiseman, P. Pantazis, B. G. Giovanella, M. A. Tainsky, A. Bradley, and L. A. Donehower.** 1993. In vitro growth characteristics of embryo fibroblasts isolated from p53-deficient mice. Oncogene **8:**2457–2467.
10. **Jacks, T., L. Remington, B. O. Williams, E. M. Schmitt, S. Halachmi, R. T. Bronson, and R. A. Weinberg.** 1994. Tumor spectrum analysis in p53 mutant mice. Curr. Biol. **4:**1–7.
11. **Jackson, M. W., and S. J. Berberich.** 2000. Mdmx protects p53 from Mdm2-mediated degradation. Mol. Cell. Biol. **20:**1001–1007.
12. **Jones, S. N., A. E. Roe, L. A. Donehower, and A. Bradley.** 1995. Rescue of embryonic lethality in Mdm2-deficient mice by absence of p53. Nature **378:** 206–208.
13. **Jones, S. N., A. T. Sands, A. R. Hancock, H. Vogel, L. A. Donehower, S. P. Linke, G. M. Wahl, and A. Bradley.** 1996. The tumorigenic potential and cell growth characteristics of p53-deficient cells are equivalent in the presence or absence of Mdm2. Proc. Natl. Acad. Sci. USA **93:**14106–14111.
14. **Kadia, M., C. Slader, and S. J. Berberich.** 2001. Regulation of p63 function by Mdm2 and Mdmx. DNA Cell Biol. **20:**321–330.
15. **Koff, A., A. Giordano, D. Desai, K. Yamashita, J. W. Harper, S. Elledge, T. Nishimoto, D. O. Morgan, B. R. Franza, and J. M. Roberts.** 1992. Formation and activation of cyclin E/CDK2 complex during the G1 phase of the human cell cycle. Science **257:**1689–1694.
16. **Levine, A. J.** 1997. p53, the cellular gatekeeper for growth and division. Cell **88:**323–331.
17. **MacCallum, D. E., T. R. Hupp, C. A. Midgley, D. Stuart, S. J. Campbell, A. Harper, F. S. Walsh, E. G. Wright, A. Balmain, D. P. Lane, and P. A. Hall.** 1996. The p53 response to ionising radiation in adult and developing murine tissues. Oncogene **13:**2575–2587.
18. **Migliorini, D., D. Danovi, E. Colombo, R. Carbone, P. G. Pelicci, and J.-C. Marine.** 2002. Hdmx recruitment into the nucleus by Hdm2 is essential for its ability to regulate p53 stability and transactivation. J. Biol. Chem. **277:** 7318–7323.
19. **Miller, F. D., C. D. Pozniak, and G. S. Walsh.** 2000. Neuronal life and death: an essential role for the p53 family. Cell Death Differ. **7:**880–888.
20. **Montes de Oca Luna, R., D. S. Wagner, and G. Lozano.** 1995. Rescue of early embryonic lethality in mdm2-deficient mice by absence of p53. Nature **378:**203–206.
21. **Nicholson, D. W., A. Ali, N. A. Thornberry, J. P. Vaillancourt, C. K. Ding, M. Gallant, Y. Gareau, P. R. Griffin, M. Labelle, Y. A. Lazebnik, et al.** 1995.

Identification and inhibition of the ICE/CED-3 protease necessary for mammalian apoptosis. Nature **376:**37–43.
22. **Ohtsubo, M., and J. M. Roberts.** 1993. Cyclin dependent regulation of G1 in mammalian fibroblasts. Science **59:**1908–1912.
23. **Ohtsubo, M., A. M. Theodoras, J. Schumacher, J. M. Roberts, and M. Pagano.** 1995. Human cyclin E, a nuclear protein essential for the G_1-to-S phase transition. Mol. Cell. Biol. **15:**2612–2624.
24. **Ongkeko, W. M., X. Q. Wang, W. Y. Siu, A. W. Lau, K. Yamashita, A. L. Harris, L. S. Cox, and R. Y. Poon.** 1999. MDM2 and MDMX bind and stabilize the p53-related protein p73. Curr. Biol. **9:**829–832.
25. **Parant, J., A. Chavez-Reyes, N. A. Little, W. Yan, V. Reinke, A. G. Jochemsen, and G. Lozano.** 2001. Rescue of embryonic lethality in *Mdm4*-null mice by loss of Trp53 suggests a non-overlapping pathway with MDM2 to regulate p53. Nat. Genet. **29:**92–95.
26. **Ramos, Y. F., R. Stad, J. Attema, L. T. Peltenburg, A. J. van der Eb, and A. G. Jochemsen.** 2001. Aberrant expression of HDMX proteins in tumor cells correlates with wild-type p53. Cancer Res. **61:**1839–1842.
27. **Roth, J., M. Dobbelstein, D. A. Freedman, T. Shenk, and A. J. Levine.** 1998. Nucleo-cytoplasmic shuttling of the hdm2 oncoprotein regulates the levels of the p53 protein via a pathway used by the human immunodeficiency virus rev protein. EMBO J. **17:**554–564.
28. **Samuels-Lev, Y., D. J. O'Connor, D. Bergamaschi, G. Trigiante, J. K. Hsieh, S. Zhong, I. Campargue, L. Naumovski, T. Crook, and X. Lu.** 2001. ASSP proteins specifically stimulate the apoptotic function of p53. Mol. Cell **8:**781–794.
29. **Sharp, D. A., S. A. Kratowicz, M. J. Sank, and D. L. George.** 1999. Stabilization of the MDM2 oncoprotein by interaction with the structurally related MDMX protein. J. Biol. Chem. **274:**38189–38196.
30. **Shvarts, A., W. T. Steegenga, N. Riteco, T. van Laar, P. Dekker, M. Bazuine, R. C. van Ham, W. van der Houven van Oordt, G. Hateboer, A. J. van der Eb, and A. G. Jochemsen.** 1996. MDMX: a novel p53-binding protein with some functional properties of MDM2. EMBO J. **15:**5349–5357.
31. **Shvarts, A., M. Bazuine, P. Dekker, Y. F. Ramos, W. T. Steegenga, G. Merckx, R. C. van Ham, W. van der Houven van Oordt, A. J. van der Eb, and A. G. Jochemsen.** 1997. Isolation and identification of the human homolog of a new p53-binding protein, Mdmx. Genomics **43:**34–42.
32. **Stad, R., N. A. Little, D. P. Xirodimas, R. Frenk, A. J. van der Eb, D. P. Lane, M. K. Saville, and A. G. Jochemsen.** 2000. Hdmx stabilizes Mdm2 and p53. J. Biol. Chem. **275:**28039–28044.
33. **Stad, R., Y. F. Ramos, N. Little, S. Grivell, J. Attema, A. J. van Der Eb, and A. G. Jochemsen.** 2001. Mdmx stabilizes p53 and Mdm2 via two distinct mechanisms. EMBO Rep. **2:**1029–1034.
34. **Tanimura, S., S. Ohtsuka, K. Mitsui, K. Shirouzu, A. Yoshimura, and M. Ohtsubo.** 1999. MDM2 interacts with MDMX through their RING finger domains. FEBS Lett. **447:**5–9.
35. **Tao, W., and A. J. Levine.** 1999. Nucleocytoplasmic shuttling of oncoprotein Hdm2 is required for Hdm2-mediated degradation of p53. Proc. Natl. Acad. Sci. USA **96:**3077–3080.
36. **Vousden, K. H.** 2000. p53: death star. Cell **103:**691–694.
37. **Yam, C. H., W. Y. Siu, T. Arooz, C. H. Chiu, A. Lau, X. Q. Wang, and R. Y. Poon.** 1999. MDM2 and MDMX inhibit the transcriptional activity of ectopically expressed SMAD proteins. Cancer Res. **59:**5075–5078.
38. **Zambrowicz, B. P., G. A. Friedrich, E. C. Buxton, S. L. Lilleberg, C. Person, and A. T. Sands.** 1998. Disruption and sequence identification of 2,000 genes in mouse embryonic stem cells. Nature **392:**608–611.